

# This&That: Language-Gesture Controlled Video Generation for Robot Planning

Boyang Wang<sup>1</sup> Nikhil Sridhar<sup>1</sup> Chao Feng<sup>1</sup> Mark Van der Merwe<sup>1</sup>

Adam Fishman<sup>2</sup> Nima Fazeli<sup>1</sup> Jeong Joon Park<sup>1</sup>

<sup>1</sup>University of Michigan <sup>2</sup>University of Washington

**Abstract:** We propose a robot learning method for communicating, planning, and executing a wide range of tasks, dubbed *This&That*. We achieve robot planning for general tasks by leveraging the power of video generative models trained on internet-scale data containing rich physical and semantic context. In this work, we tackle three fundamental challenges in video-based planning: 1) unambiguous task communication with simple human instructions, 2) controllable video generation that respects user intents, and 3) translating visual planning into robot actions. We propose language-gesture conditioning to generate videos, which is both simpler and clearer than existing language-only methods, especially in complex and uncertain environments. We then suggest a behavioral cloning design that seamlessly incorporates the video plans. *This&That* demonstrates state-of-the-art effectiveness in addressing the above three challenges, and justifies the use of video generation as an intermediate representation for generalizable task planning and execution. Project website: <https://cfeng16.github.io/this-and-that/>.

**Keywords:** Video-based Planning, Behavioral Cloning, Generative Model

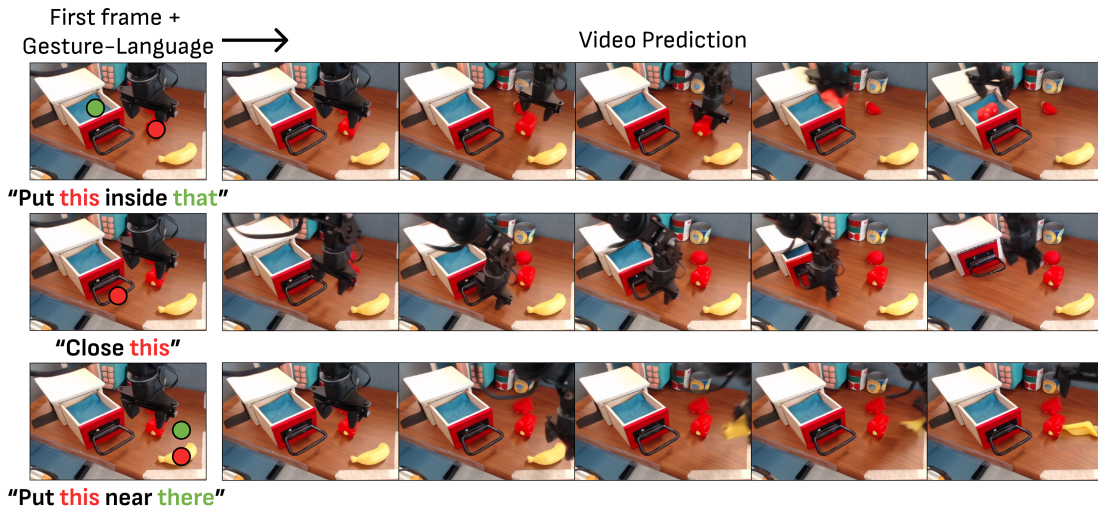


Figure 1: **Video generation for robot planning.** Using the same initial frame, our video diffusion model can effectively generate various action sequences, each conditioned on different pairs of gestures and text prompts. Our approach accommodates simple deictic language such as *this* and *that*.

## 1 Introduction

When we instruct other people to perform a task, we often point to the targets and say things like: “Give me that glass.”, or “Put this there.”. Such simple language-gesture instructions can be more effective in communicating tasks than verbally describing them without gestures. For example, a

verbal instruction – “Give me the blue glass located on the third row of the wooden cabinet.” – can be verbose and ambiguous. The combination of pointing gestures and *deictic* words such as “this” and “that” is convenient and clear at the same time, so it is used widely across cultures. Wouldn’t it be amazing if we could control robots on a wide range of tasks using these simple language-gesture commands? Through this work, we strive to achieve exactly *that*.

Our proposed framework, dubbed *This&That*, includes a controllable video generation module and a video-driven robot execution module. We build our video generator on top of a recent large-scale, open-vocabulary text-to-video diffusion models [1], which we fine-tune to adapt to our robotics setups. Our refined video diffusion model (VDM) is conditioned on input language describing the task using deictic words such as “this” and “there,” as well as input gestures represented as the 2D locations in the first frame image corresponding to the language. We introduce novel techniques to effectively incorporate the multi-modal conditionings, leading to SOTA-quality videos that closely align with human intentions even for uncertain tasks in complex scenes.

Inspired by recent developments, we consider the video generator as a generalizable planner that envisions the change of environment for a wide range of tasks. Here, the predicted video is a guide for robot actions, and the execution module only has to follow the predicted video. Unlike existing video-based approaches that either simplify the action space [2] or devise special inverse dynamics models [3], we incorporate the ability to follow video predictions into well-established behavioral cloning (BC) architectures such as the Action Chunking Transformer [4]. Our BC-based execution module efficiently cross-attends to the video frames to unify video-based planning and manipulation.

We conduct experiments on the Bridge video datasets [5, 6] and IsaacGym simulation datasets, where we deploy virtual robot policy rollouts. Our experiments include a wide range of open-vocabulary tasks within complex and uncertain environments. The results demonstrate that our *This&That* framework produces higher quality videos with superior alignment to user intentions than prior works. Our behavioral cloning experiments in simulation environments show the benefits of our proposed language-gesture commands and further justify the use of conditional video predictions for multi-task policy learning. Overall, we claim the following two contributions:

- We propose language-gesture interactions with robots to achieve simple yet effective human-robot communication. Moreover, we develop language-gesture conditioned video generation techniques that lead to high-quality video-based planning that better aligns with user intentions than previous language-only methods.
- We devise a video-conditioned behavioral cloning architecture to integrate the generated video predictions with live observations for multi-task robot policy learning.

## 2 Related work

**2.1. Imitation Learning:** Imitation learning is a technique to learn robotic behavior from expert demonstration. Behavior cloning (BC) casts this task as supervised learning, where the aim is to train a policy to directly mimic the expert’s actions. Recently, BC has demonstrated strong performance in learning complex, dextrous robot skills [7, 8, 4, 9, 10]. While some BC policies rely solely on the robot’s state, adding goal information to the policy allows the robot to disambiguate between tasks [11]. Goals can be expressed as language instruction [9, 12, 13, 14, 15], images [16], or even sketches [17]. When visual goals are expressed as a single image, as in [18, 9, 19], the goals can be ambiguous and the models have a tendency to overfit. Instead, we represent goals as a dense sequence of images, predicted by a video diffusion model. By providing intermediate goal information, we find this formulation to better aid the policy to actually reach the long-term goal.

**2.2. Video Diffusion Models:** A Video Diffusion Model (VDM) aims to generate temporally consistent and high-fidelity videos [20, 21, 22] that align the provided conditions, which may include image [23], text [24], audio [25], segmentation [26, 27, 28], camera pose [29, 30], and human pose [31, 32] and so on. These conditions can be combined to facilitate highly controllable video generation outcomes.

In VDM, significant attention has been given to motion and camera control. MotionCtrl [33] introduces object motion control by learning sparse optical flow change and a self-attention mechanism in the temporal layers to learn camera motion. DragAnything [26] and Follow-Your-Click [27] leverage segmentation masks to identify target objects and provide complete trajectory data to each frame during training, thus controlling object motion in generated videos. SparseCtrl [28] introduces channel-wise concatenation to address the challenges posed by sparse temporal conditions during the inference stage. However, these methods typically require either dense spatial or dense temporal information, or both, for effective temporal control. In contrast, our approach requires minimal temporal control inputs, as sparse as two points, with all other information such as trajectory inferred by the model based on learned statistical patterns.

**2.3. Video Diffusion Models in Robotics:** Considerable progress has been made in advancing VDM for use in downstream robotics application [34, 35, 36, 3, 2], yet both the mechanisms of directed video prediction and video-conditioned control are still under-explored. UniPi [36] and UniSim [3] demonstrate how basic image and text-to-video generation can simulate robotic interactions in real-world scenes, and how the generated videos can be converted into robot actions through inverse dynamics modeling. However, their VDM formulation cannot accurately predict behavior in ambiguous scenes, a problem we address by conditioning the video on gesture as well. AVDC [2] extracts optical flow information of the generated videos and depth information and converts them into a discrete action.

### 3 Overview

Our proposed *This&That* framework is composed of two components: language-gesture-conditioned video generation and video-based robot planning. In Sec. 4, we introduce our video diffusion model built on top of a large video model. Notably, we use the language-gesture conditioning to provide user-friendly control (Sec 4.2). In Sec. 5, we introduce our behavioral cloning approach which references the generated video for executing the visual plans. In the experiment section (Sec. 6), we mainly prove the better user alignment of the language-gesture conditioning and the ability to translate a video into robot actions in simulated environments.

## 4 Language-Gesture Conditioned Video Diffusion Models

**Preliminaries** Recent video diffusion models (VDM) adopt training and sampling techniques similar to image diffusion models. During the forward diffusion, VDMs add Gaussian noise of random level to the video frames, training the model to predict this noise. In the reverse phase, VDMs use a Markov chain of iterative steps, where the trained neural network denoises the current frames. Message passing in both temporal and spatial dimensions is crucial for generating consistent frames.

Current leading generative methods [1, 37] often operate in the latent space instead of the raw pixel space to reduce computational demands. Latent VDMs convert video frames to latent space using an encoder  $\mathcal{E}$  during denoising and revert these latents to pixel space using a decoder  $\mathcal{D}$  post-denoising.

**Fine-tuning Large Video Models** In this work, we use pre-trained Stable Video Diffusion (SVD) [1] as our foundational latent VDM, designed for open-vocabulary video generation due to its training on high-quality internet-scale data. Our VDM generates  $T$  video frames from an initial frame  $I_0$ , aiming to learn a conditional joint distribution  $p_{\theta}(I_1, \dots, I_T | I_0, C_{\text{text}}, C_{\text{gest}})$  with added language and gesture conditions. We fine-tune our VDM in two phases: first by fine-tuning SVD with text and first frames on a robotics dataset, then making architectural modifications and further refining with gesture conditioning.

### 4.1 Language-Conditioned Finetuning

Most large VDMs, such as SVD, are trained on general, broad datasets and are not directly suitable for robotic tasks. To address this, we retain SVD’s core structure but initially fine-tune it on robotics videos. We enhance SVD by incorporating language description  $C_{\text{text}}$  and first frame  $I_0$  conditionings through Feature-wise Linear Modulation (FiLM) [38], modulating intermediate

features using parameters derived from cross-attention between language and image tokens, with token extraction facilitated by the CLIP [39] encoder.

During training, we introduce Gaussian noise to frames  $I_{0:T}$  and optimize the model using the noise reconstruction loss, conditioned on the initial frame and text. Considering the nature of robotics videos, which mark clear start and end of tasks, we uniformly subsample the sequence to compile  $T$  target frames per video ( $T$  typically from 14 to 25). For detailed information on data processing and fine-tuning methods, we highly recommend readers refer to the supplementary material.

## 4.2 Gesture-Conditioned Training and Inference

We use a combination of language and pointing gestures marked as 2D locations on the first frame to intuitively control video generation. To condition video generation with these gestures, we adapt our VDM architecture (Fig. 2) to include a supplementary network structure parallel to our fine-tuned diffusion UNet, following ControlNet [40] for image-conditioned generation. At this stage, we freeze the diffusion UNet weights and train only the new gesture conditioning branch.

We find that naïvely applying the ControlNet scheme to our use case does not ensure that the video follows the gesture, due to the spatial and temporal sparsity of the conditioning information. Specifically, the 2D gesture locations usually appear only in two frames, leaving the other frames and locations unconstrained, which led ControlNet to ignore the conditioning. Furthermore, the 2D gesture input alone does not fully define the task; it needs to be interpreted alongside the generated video and the action-oriented language of the text prompt, such as *flip this cloth from here*.

To resolve these issues, inspired by [27], we augment the gesture conditioning branch inputs with the first frame  $I_0$ , the current noisy image  $\epsilon_t$  at each denoising step  $t$ , and the sparse gesture images  $C_{\text{gest}}$ . We also modulate the branch with the text prompt. These adjustments ensure dense input signals across the conditioning branch, allowing gestures to be integrated meaningfully with current video content and language. Finally, images  $I_0$  and  $C_{\text{gest}}$  are processed with a pre-trained encoder  $\mathcal{E}$  from StableDiffusion, with random masking  $\mathcal{M}_p$  applied to the image latent, form the inputs to the conditioning branch.

Since most robotics video dataset lacks ground truth gesture locations, we automatically annotate them by detecting the 2D gripper location when it opens and closes, identifying target gesture points. Further annotation details are in the supplementary. After obtaining these locations, we enhance the spatial signal by applying a 2D Gaussian filter to dilate the points, following [33]. For tasks like opening a door, where only the initial contact point is relevant, we only consider one gesture point.

## 5 Video-Conditioned Behavioral Cloning

We want a policy  $\pi(\cdot)$  to translate frames  $\mathcal{I} = [I_0, \dots, I_T]$  from the video plan into executable robot actions. For this, we developed DiVA (**D**iffusion **V**ideo to **A**ction), a behavioral cloning model referencing the entire or partial subset of the predicted video sequence (see Fig. 3). DiVA, based on a Transformer encoder-decoder architecture similar to ACT [4], is trained to predict the next chunk of actions  $a_{t+k}$  based on the current image observation  $o_t$ , the robot’s end-effector pose  $s_t$ , and the video sequence  $\tau$ : DiVA learns to sample from the conditional action distribution  $\pi_{\theta}(a_{t:t+k}|o_t, s_t, \tau)$ . For our action space, we use a 6D delta end-effector pose expressed in the end-effector frame.

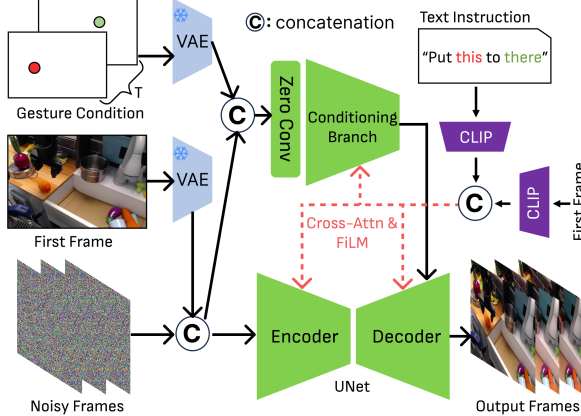


Figure 2: **Overview of video diffusion model.** Our video diffusion model architecture with the first frame image and language-gesture conditioning.

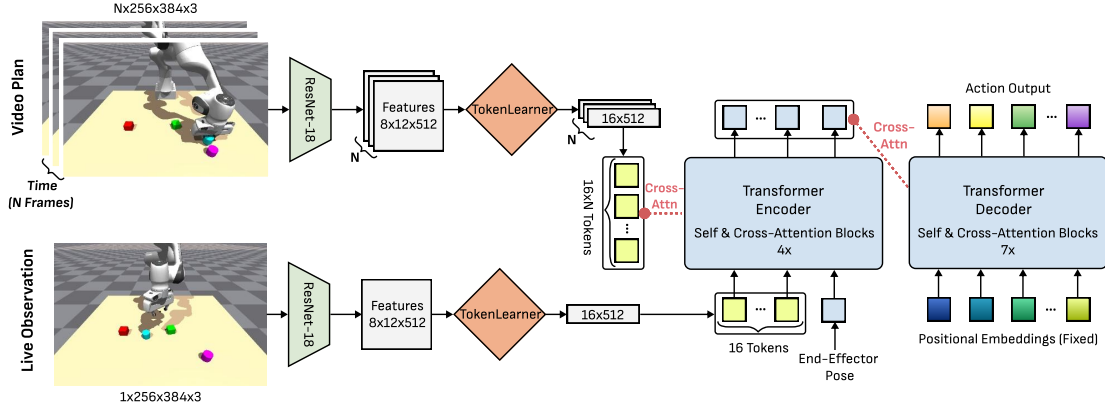


Figure 3: **Video-conditioned behavioral cloning architecture.** Our Diffusion Video to Action (DiVA) model compresses the live and predicted video frames using TokenLearner [41]. DiVA uses Transformer encoder-decoder backbone and references video plan tokens with cross-attention.

| Methods           | FID↓         | FVD↓         | PSNR↑        | SSIM↑        | LPIPS↓       |
|-------------------|--------------|--------------|--------------|--------------|--------------|
| SVD [1]           | 29.49        | 657.49       | 11.17        | 0.285        | 0.473        |
| StreamingT2V [24] | 42.57        | 780.81       | 10.48        | 0.303        | 0.570        |
| DragAnything [26] | 34.38        | 764.58       | 9.88         | 0.283        | 0.590        |
| AVDC [2]          | 163.93       | 1512.25      | 19.43        | 0.649        | 0.517        |
| <b>Ours</b>       | <b>17.28</b> | <b>84.58</b> | <b>20.03</b> | <b>0.761</b> | <b>0.137</b> |

Table 1: **Quantitative video quality analysis on Bridge dataset.** The best is highlighted.

Given the video frames  $\mathcal{I}$  and the live image frame  $o_t$ , we first convert them into latent embeddings using the ImageNet pre-trained ResNet-18 which is fine-tuned during training. Since we are dealing with a potentially large number of images in the predicted video, we apply TokenLearner [41] to compress the size of the embeddings to only 16 tokens per image. As shown in Fig. 3, we process live image tokens with a Transformer [42] encoder that cross-attends to all video frame tokens augmented with positional encoding. Finally, a Transformer decoder is used to convert a fixed positional embedding into action chunk outputs, by cross-attending to the encoder output. Details of the architecture and additional configurations can be found in the supplementary material.

During training, we use  $N$  evenly spaced images from each demonstration as ground-truth goals for  $\mathcal{I}$ . In inference, these are replaced by outputs from our video diffusion model. Initial experiments revealed a domain gap between ground truth and model-generated goals, leading to errors potentially due to small temporal misalignments. To enhance robustness, we introduce temporal noise by randomly sampling an image from  $N$  even groups of ground-truth images to form the goal sequence during training. We discuss the effect of varying  $N$  in the supplementary document.

## 6 Experiments

We conduct a series of experiments to show the superior user alignment of our *This&That* framework, focusing on the accuracy of video generation and the translation of video plans into robot actions. Specifically, our main experiments aim to 1) show realistic, user-aligned video generations, 2) assess the effectiveness of our language-gesture conditioning, and 3) evaluate the successful integration of predicted video plans with a behavior cloning algorithm in synthetic rollouts.

### 6.1 Video Generation Experiments and Comparisons

**Bridge Dataset** We evaluate our video generation framework with the Bridge V1 [6] and V2 [5] datasets, which are widely-used real robot datasets with human demonstrations. The Bridge datasets feature complex real-world scenes and tasks, focusing on household environments such as kitchens, laundry areas, and desk tops. We solely use the frontal view scenes and prune both short and long sequences for simplicity of training. Across V1 and V2, we obtain 25,767 videos for the initial finetuning (Sec. 4.1) and gather 14,735 videos for the gesture conditioned training (Sec. 4.2), after filtering out videos where the automatic annotation failed. Refer to the supplementary for details.



Figure 4: **Video-based Planning Qualitative Results.** We present three examples to compare *This&That* with AVDC [2]. The gesture locations are overlaid in the leftmost frame. Our method can generate action sequences effectively with higher visual quality, even when using deictic words.

**Evaluating Video Prediction Qualities** To assess the quality of our video predictions for a robotics setup, we compare against the most recent video synthesis methods in Image-to-Video (SVD [1]), Image-Text-to-Video (StreamingT2V [24]), and Image-Gesture-to-Video (DragAnything [26]). We also compare with the SOTA open-source VDM of robotics, AVDC [2] (Image-Text-to-Video) which is trained on the entire Bridge dataset.

We evaluate these methods on the 646 test videos of the Bridge dataset using the Frchet Inception Distance (FID) [43] and Frchet Video Distance (FVD) [44] to evaluate visual and temporal generation quality. Moreover, we compute loss against the ground truth images using pixel-wise and perceptual metrics (PSNR, SSIM, and LPIPS [45]). As shown in Tab. 1, our language-gesture conditioned VDM demonstrates its superior visual realism and temporal alignment against the baselines, including AVDC which has seen these test videos during training.

**User Alignment Study** We conduct a human study to evaluate the alignment of the generated videos. To this end, we explain our ground truth intention to the participants (using both language and gesture) and ask whether the given video aligns with the intention. Here, we test AVDC and our trained VDM models with different combinations of input conditioning: vision (first frame image), language, and gesture. Moreover, we test two forms of language conditioning for the same model weight: *regular* language from the original Bridge dataset and our *deictic* format. Moreover, we select 24 test sequences from Bridge and categorize them into four robotics tasks: *pick and place*, *stacking*, *folding*, and *open or close*.

The results in Tab. 2 and Fig. 4 demonstrate a significant improvement in alignment for the language-gesture conditioning, outperforming baselines. Using ambiguous deictic language, e.g., “this” and



Figure 5: **Limitation of gesture-only conditioning.** 2D gestures can suffer from 3D ambiguity as an image perspective coordinate does not fully decide a 3D coordinate (see (a) and (b)). A simple language cue can break this ambiguity as shown in (c). Moreover, we empirically observe higher visual quality for language-gesture models, likely due to reduced uncertainty during training.

| Modality         | Success Rate (%) |              |              |              |              |              |              |              |              |              |
|------------------|------------------|--------------|--------------|--------------|--------------|--------------|--------------|--------------|--------------|--------------|
|                  | Pick&Place       |              | Stacking     |              | Folding      |              | Open/Close   |              | Average      |              |
|                  | Regular text     | Deictic text | Regular text | Deictic text | Regular text | Deictic text | Regular text | Deictic text | Regular text | Deictic text |
| Vision (V.)      | 0.0              | -            | 6.6          | -            | 11.1         | -            | 60.0         | -            | 16.7         | -            |
| AVDC (V.+Lang.)  | 8.3              | 8.3          | 0.0          | 0.0          | 5.6          | 5.6          | 40.0         | 40.0         | 12.5         | 12.5         |
| V.+Lang.         | 37.5             | 4.2          | 26.7         | 6.6          | 50.0         | 33.3         | <b>100.0</b> | 66.7         | 51.4         | 25.0         |
| V.+Gesture       | 58.3             | -            | <u>66.7</u>  | -            | 55.6         | -            | <b>100.0</b> | -            | 68.1         | -            |
| V.+Lang.+Gesture | <b>95.8</b>      | <u>91.6</u>  | <b>80.0</b>  | <u>66.7</u>  | <u>88.9</u>  | <b>94.4</b>  | <b>100.0</b> | <u>93.3</u>  | <b>91.7</b>  | <u>87.5</u>  |

Table 2: **User alignment evaluation of video generation.** We conduct a user study to evaluate whether the videos generated from various conditioning modalities align with the ground truth intentions. Regular text refers to the prompt provided by the dataset and Deictic indicates the post-processed ambiguous prompt. For *V.* and *V.+Gesture*, no text conditioning is used. The best for each task is highlighted and the second best is underlined.

“there” does not significantly hurt user alignment scores while making commands much simpler from the user side. Our *this&that* method shines in complex and uncertain tasks such as *pick and place*. We do note that for the *open and close* task that involves one specific handle to manipulate, all methods work effectively since there is little to no ambiguity and only a simple command is necessary. Finally, we highlight, in Fig. 5, where gesture alone might fail to specify a task mainly due to the inherent ambiguity of the 2D gesture location in the 3D space.

## 6.2 Synthetic Rollout Experiments

We design a simulation environment using Isaac Gym [46] to evaluate our method’s performance in translating video plans into robot actions under significant amounts of ambiguity. We set four blocks on a tabletop environment and prepare pick-and-place tasks by relating two randomly selected objects in diverse ways (e.g., *place the blue cube in front of the orange cylinder*). We use a hand-scripted policy to obtain ground truth trajectories and train our VDM and DiVA policy models using programmatically generated conditionings. During testing, we further stress-test the methods by introducing out-of-distribution scenes that contain identical objects in identical colors.

The results in Tab. 3 and Fig. 6 again show that our method conditioned on language and gesture outperforms the policy relying solely on language for both in and out of distribution cases. We also modify ACT [4] to consume the language and gesture conditioning directly and find that it underperforms compared to our main model (refer to supplementary for details). These results highlight the effectiveness and robustness of our language-gesture-guided VDM to accurately indicate the goals of the policy.

## 7 Limitations

Although our model generates high-fidelity videos, object shapes often change over time, likely due to the lack of 3D geometric constraints. Our predictions are limited to short, modular tasks; extending them to longer tasks (e.g., cooking) with multi-modal instructions present a significant opportunity. Moreover, our automatic gesture labeling is susceptible to image artifacts such as motion blur.

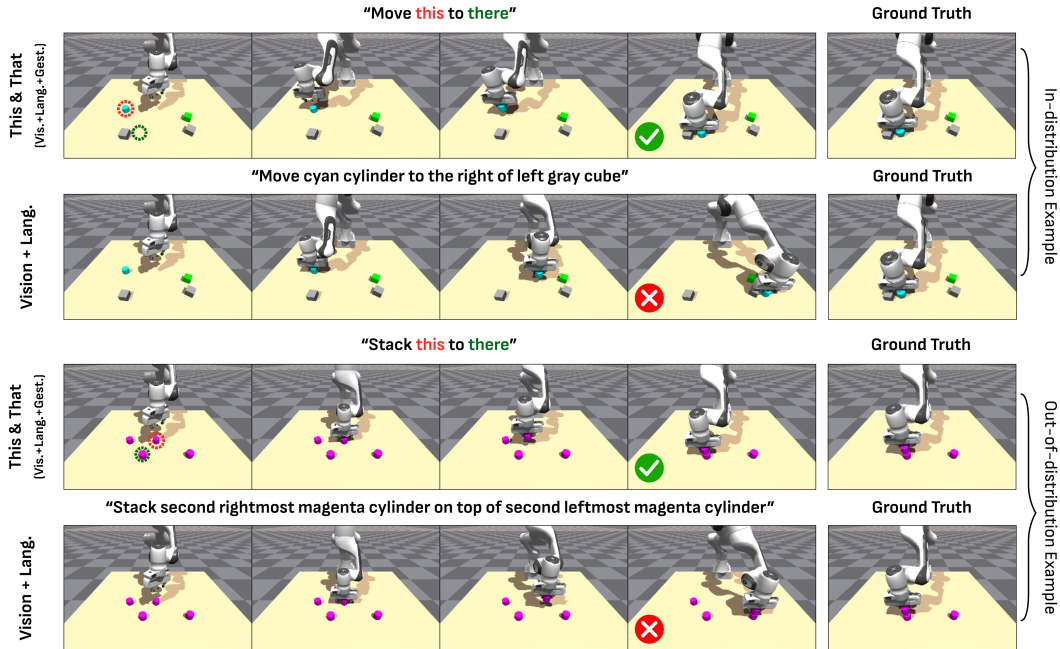


Figure 6: **Simulation Rollout Qualitative Comparison.** We compare our language-gesture model against the video-based baseline conditioned solely on language. The language-only VDM struggles to interpret complex text instructions and resolve scene ambiguities. In contrast, our model effectively translates user intentions into actions, even with the use of simple deictic words.

| Goal-Conditioning           | Success Rate (%) |               |                 |
|-----------------------------|------------------|---------------|-----------------|
|                             | Pick Success     | Place Success | Overall Success |
| ACT (Vanilla)               | 5/3              | 0/33          | 0/1             |
| ACT(Language)               | 3/3              | 0/0           | 0/0             |
| ACT(Lang.+Gesture)          | 57/56            | 61/63         | 35/35           |
| Video-based (Langauge)      | 96/56            | 89/41         | 85/23           |
| Video-based (Lang.+Gesture) | <b>97/89</b>     | <b>96/93</b>  | <b>93/83</b>    |

Table 3: **A quantitative comparison on synthetic robot rollouts.** We assess video-based methods (DiVA) and goal-conditioned behavioral cloning methods (ACT) in simulation. Pick success indicates whether the object of interest was grasped and picked up successfully while place success indicates whether the object was moved to the target location, provided it was picked successfully. The overall success is multiplied by the pick success and place success rate. The two numbers represent results on in-distribution and out-of-distribution scenes, respectively. The best is highlighted.

**Transfer to Real Robots.** Finally, our video-based behavioral cloning experiments are currently limited to simulated environments. While we achieved state-of-the-art generation results on Bridge videos, the standard real datasets for this task, we could not test with real robots due to the unavailability of the WidowX 250 arm at our academic facility. However, existing research involving the Bridge data has consistently shown the successful transfer of generated video plans to real robot manipulations, and that real-world performance closely correlates with simulated results. Based on these findings, our advancements in video generative models and behavioral cloning represent fundamental contributions to video-based real robot planning.

## 8 Conclusion

In this work, we present *This&That*, a framework that combines the power of visual generative models and imitation learning for effective task communication and planning. *This&That* leverages a language-gesture conditioned video generative model as an intermediate planner and uses a video-based behavioral cloning model that elegantly combines the predicted frames and live observation



into actions. Our experiments demonstrate that our generated videos and their subsequent rollouts align exceptionally well with user’s intentions, suggesting an exciting new direction toward multi-task human-robot collaborations.

## Acknowledgement

We thank Xuweiyi Chen and Haoran Zhang for the helpful discussion.

## References

- [1] A. Blattmann, T. Dockhorn, S. Kulal, D. Mendelevitch, M. Kilian, D. Lorenz, Y. Levi, Z. English, V. Voleti, A. Letts, et al. Stable video diffusion: Scaling latent video diffusion models to large datasets. *arXiv preprint arXiv:2311.15127*, 2023.
- [2] P.-C. Ko, J. Mao, Y. Du, S.-H. Sun, and J. B. Tenenbaum. Learning to act from actionless videos through dense correspondences. *arXiv preprint arXiv:2310.08576*, 2023.
- [3] M. Yang, Y. Du, K. Ghasemipour, J. Tompson, D. Schuurmans, and P. Abbeel. Learning interactive real-world simulators. *arXiv preprint arXiv:2310.06114*, 2023.
- [4] T. Z. Zhao, V. Kumar, S. Levine, and C. Finn. Learning fine-grained bimanual manipulation with low-cost hardware. *arXiv preprint arXiv:2304.13705*, 2023.
- [5] H. R. Walke, K. Black, T. Z. Zhao, Q. Vuong, C. Zheng, P. Hansen-Estruch, A. W. He, V. Myers, M. J. Kim, M. Du, et al. Bridgedata v2: A dataset for robot learning at scale. In *Conference on Robot Learning*, pages 1723–1736. PMLR, 2023.
- [6] F. Ebert, Y. Yang, K. Schmeckpeper, B. Bucher, G. Georgakis, K. Daniilidis, C. Finn, and S. Levine. Bridge data: Boosting generalization of robotic skills with cross-domain datasets, 2021.
- [7] M. Shridhar, L. Manuelli, and D. Fox. Perceiver-actor: A multi-task transformer for robotic manipulation, 2022.
- [8] C. Chi, S. Feng, Y. Du, Z. Xu, E. Cousineau, B. Burchfiel, and S. Song. Diffusion policy: Visuomotor policy learning via action diffusion. In *Proceedings of Robotics: Science and Systems (RSS)*, 2023.
- [9] A. Brohan, N. Brown, J. Carbajal, Y. Chebotar, J. Dabis, C. Finn, K. Gopalakrishnan, K. Hausman, A. Herzog, J. Hsu, J. Ibarz, B. Ichter, A. Irpan, T. Jackson, S. Jesmonth, N. J. Joshi, R. Julian, D. Kalashnikov, Y. Kuang, I. Leal, K.-H. Lee, S. Levine, Y. Lu, U. Malla, D. Manjunath, I. Mordatch, O. Nachum, C. Parada, J. Peralta, E. Perez, K. Pertsch, J. Quiambao, K. Rao, M. Ryoo, G. Salazar, P. Sanketi, K. Sayed, J. Singh, S. Sontakke, A. Stone, C. Tan, H. Tran, V. Vanhoucke, S. Vega, Q. Vuong, F. Xia, T. Xiao, P. Xu, S. Xu, T. Yu, and B. Zitkovich. Rt-1: Robotics transformer for real-world control at scale, 2023.
- [10] P. Florence, C. Lynch, A. Zeng, O. Ramirez, A. Wahid, L. Downs, A. Wong, J. Lee, I. Mordatch, and J. Tompson. Implicit behavioral cloning. *Conference on Robot Learning (CoRL)*, 2021.
- [11] B. Argall, S. Chernova, M. Veloso, and B. Browning. A survey of robot learning from demonstration. *Robotics and Autonomous Systems*, 57:469–483, 05 2009. doi:10.1016/j.robot.2008.10.024.
- [12] C. Lynch, A. Wahid, J. Tompson, T. Ding, J. Betker, R. Baruch, T. Armstrong, and P. Florence. Interactive language: Talking to robots in real time, 2022.
- [13] S. Karamcheti, S. Nair, A. S. Chen, T. Kollar, C. Finn, D. Sadigh, and P. Liang. Language-driven representation learning for robotics, 2023.

- [14] C. Lynch and P. Sermanet. Language conditioned imitation learning over unstructured data, 2021.
- [15] L. Shao, T. Migimatsu, Q. Zhang, K. Yang, and J. Bohg. Concept2robot: Learning manipulation concepts from instructions and human demonstrations. In *Proceedings of Robotics: Science and Systems (RSS)*, 2020.
- [16] M. Danielczuk, A. Kurenkov, A. Balakrishna, M. Matl, D. Wang, R. Martin-Martin, A. Garg, S. Savarese, and K. Goldberg. Mechanical search: Multi-step retrieval of a target object occluded by clutter. In *2019 International Conference on Robotics and Automation (ICRA)*. IEEE, May 2019. doi:10.1109/icra.2019.8794143. URL <http://dx.doi.org/10.1109/ICRA.2019.8794143>.
- [17] P. Sundaresan, Q. Vuong, J. Gu, P. Xu, T. Xiao, S. Kirmani, T. Yu, M. Stark, A. Jain, K. Hausman, D. Sadigh, J. Bohg, and S. Schaal. Rt-sketch: Goal-conditioned imitation learning from hand-drawn sketches, 2024.
- [18] E. Jang, A. Irpan, M. Khansari, D. Kappler, F. Ebert, C. Lynch, S. Levine, and C. Finn. Bc-z: Zero-shot task generalization with robotic imitation learning, 2022.
- [19] K. Burns, T. Yu, C. Finn, and K. Hausman. Robust manipulation with spatial features. In *CoRL 2022 Workshop on Pre-training Robot Learning*, 2022. URL <https://openreview.net/forum?id=X7beXNWxYP>.
- [20] U. Singer, A. Polyak, T. Hayes, X. Yin, J. An, S. Zhang, Q. Hu, H. Yang, O. Ashual, O. Gafni, et al. Make-a-video: Text-to-video generation without text-video data. *arXiv preprint arXiv:2209.14792*, 2022.
- [21] W. Menapace, A. Siarohin, I. Skorokhodov, E. Deyneka, T.-S. Chen, A. Kag, Y. Fang, A. Stoliar, E. Ricci, J. Ren, et al. Snap video: Scaled spatiotemporal transformers for text-to-video synthesis. *arXiv preprint arXiv:2402.14797*, 2024.
- [22] W. Ren, H. Yang, G. Zhang, C. Wei, X. Du, S. Huang, and W. Chen. Consisti2v: Enhancing visual consistency for image-to-video generation. *arXiv preprint arXiv:2402.04324*, 2024.
- [23] Y. Zhou, D. Zhou, M.-M. Cheng, J. Feng, and Q. Hou. Storydiffusion: Consistent self-attention for long-range image and video generation. *arXiv preprint arXiv:2405.01434*, 2024.
- [24] R. Henschel, L. Khachatryan, D. Hayrapetyan, H. Poghosyan, V. Tadevosyan, Z. Wang, S. Navasardyan, and H. Shi. Streamingt2v: Consistent, dynamic, and extendable long video generation from text. *arXiv preprint arXiv:2403.14773*, 2024.
- [25] L. Tian, Q. Wang, B. Zhang, and L. Bo. Emo: Emote portrait alive-generating expressive portrait videos with audio2video diffusion model under weak conditions. *arXiv preprint arXiv:2402.17485*, 2024.
- [26] W. Wu, Z. Li, Y. Gu, R. Zhao, Y. He, D. J. Zhang, M. Z. Shou, Y. Li, T. Gao, and D. Zhang. Draganything: Motion control for anything using entity representation. *arXiv preprint arXiv:2403.07420*, 2024.
- [27] Y. Ma, Y. He, H. Wang, A. Wang, C. Qi, C. Cai, X. Li, Z. Li, H.-Y. Shum, W. Liu, et al. Follow-your-click: Open-domain regional image animation via short prompts. *arXiv preprint arXiv:2403.08268*, 2024.
- [28] Y. Guo, C. Yang, A. Rao, M. Agrawala, D. Lin, and B. Dai. Sparsectrl: Adding sparse controls to text-to-video diffusion models. *arXiv preprint arXiv:2311.16933*, 2023.
- [29] H. He, Y. Xu, Y. Guo, G. Wetzstein, B. Dai, H. Li, and C. Yang. Cameractrl: Enabling camera control for text-to-video generation. *arXiv preprint arXiv:2404.02101*, 2024.

- [30] Z. Kuang, S. Cai, H. He, Y. Xu, H. Li, L. Guibas, and G. Wetzstein. Collaborative video diffusion: Consistent multi-video generation with camera control. *arXiv preprint arXiv:2405.17414*, 2024.
- [31] S. Zhu, J. L. Chen, Z. Dai, Y. Xu, X. Cao, Y. Yao, H. Zhu, and S. Zhu. Champ: Controllable and consistent human image animation with 3d parametric guidance. *arXiv preprint arXiv:2403.14781*, 2024.
- [32] L. Hu, X. Gao, P. Zhang, K. Sun, B. Zhang, and L. Bo. Animate anyone: Consistent and controllable image-to-video synthesis for character animation. *arXiv preprint arXiv:2311.17117*, 2023.
- [33] Z. Wang, Z. Yuan, X. Wang, T. Chen, M. Xia, P. Luo, and Y. Shan. Motionctrl: A unified and flexible motion controller for video generation. *arXiv preprint arXiv:2312.03641*, 2023.
- [34] Y. Du, S. Yang, B. Dai, H. Dai, O. Nachum, J. Tenenbaum, D. Schuurmans, and P. Abbeel. Learning universal policies via text-guided video generation. *Advances in Neural Information Processing Systems*, 36, 2024.
- [35] S. Zhou, Y. Du, J. Chen, Y. Li, D.-Y. Yeung, and C. Gan. Robodreamer: Learning compositional world models for robot imagination. *arXiv preprint arXiv:2404.12377*, 2024.
- [36] Y. Du, M. Yang, P. Florence, F. Xia, A. Wahid, B. Ichter, P. Sermanet, T. Yu, P. Abbeel, J. B. Tenenbaum, et al. Video language planning. *arXiv preprint arXiv:2310.10625*, 2023.
- [37] R. Rombach, A. Blattmann, D. Lorenz, P. Esser, and B. Ommer. High-resolution image synthesis with latent diffusion models. In *Proceedings of the IEEE/CVF conference on computer vision and pattern recognition*, pages 10684–10695, 2022.
- [38] E. Perez, F. Strub, H. De Vries, V. Dumoulin, and A. Courville. Film: Visual reasoning with a general conditioning layer. In *Proceedings of the AAAI conference on artificial intelligence*, volume 32, 2018.
- [39] A. Radford, J. W. Kim, C. Hallacy, A. Ramesh, G. Goh, S. Agarwal, G. Sastry, A. Askell, P. Mishkin, J. Clark, et al. Learning transferable visual models from natural language supervision. In *International conference on machine learning*, pages 8748–8763. PMLR, 2021.
- [40] L. Zhang, A. Rao, and M. Agrawala. Adding conditional control to text-to-image diffusion models. In *Proceedings of the IEEE/CVF International Conference on Computer Vision*, pages 3836–3847, 2023.
- [41] M. S. Ryoo, A. Piergiovanni, A. Arnab, M. Dehghani, and A. Angelova. Tokenlearner: What can 8 learned tokens do for images and videos? *arXiv preprint arXiv:2106.11297*, 2021.
- [42] A. Vaswani, N. Shazeer, N. Parmar, J. Uszkoreit, L. Jones, A. N. Gomez, Ł. Kaiser, and I. Polosukhin. Attention is all you need. *Advances in neural information processing systems*, 30, 2017.
- [43] M. Seitzer. pytorch-fid: FID Score for PyTorch. <https://github.com/mseitzer/pytorch-fid>, 2020.
- [44] T. Unterthiner, S. Van Steenkiste, K. Kurach, R. Marinier, M. Michalski, and S. Gelly. Towards accurate generative models of video: A new metric & challenges. *arXiv preprint arXiv:1812.01717*, 2018.
- [45] R. Zhang, P. Isola, A. A. Efros, E. Shechtman, and O. Wang. The unreasonable effectiveness of deep features as a perceptual metric. In *Proceedings of the IEEE conference on computer vision and pattern recognition*, pages 586–595, 2018.

- [46] V. Makoviychuk, L. Wawrzyniak, Y. Guo, M. Lu, K. Storey, M. Macklin, D. Hoeller, N. Rudin, A. Allshire, A. Handa, et al. Isaac gym: High performance gpu-based physics simulation for robot learning. *arXiv preprint arXiv:2108.10470*, 2021.
- [47] A. Kirillov, E. Mintun, N. Ravi, H. Mao, C. Rolland, L. Gustafson, T. Xiao, S. Whitehead, A. C. Berg, W.-Y. Lo, et al. Segment anything. In *Proceedings of the IEEE/CVF International Conference on Computer Vision*, pages 4015–4026, 2023.
- [48] T. Karras, M. Aittala, T. Aila, and S. Laine. Elucidating the design space of diffusion-based generative models. *Advances in Neural Information Processing Systems*, 35:26565–26577, 2022.
- [49] Z. Dai, Z. Zhang, Y. Yao, B. Qiu, S. Zhu, L. Qin, and W. Wang. Animateanything: Fine-grained open domain image animation with motion guidance. *arXiv e-prints*, pages arXiv–2311, 2023.
- [50] J. L. Ba, J. R. Kiros, and G. E. Hinton. Layer normalization. *arXiv preprint arXiv:1607.06450*, 2016.
- [51] J. Redmon, S. Divvala, R. Girshick, and A. Farhadi. You only look once: Unified, real-time object detection. In *Proceedings of the IEEE conference on computer vision and pattern recognition*, pages 779–788, 2016.
- [52] J. Yang, M. Gao, Z. Li, S. Gao, F. Wang, and F. Zheng. Track anything: Segment anything meets videos, 2023.
- [53] I. Loshchilov and F. Hutter. Decoupled weight decay regularization. *arXiv preprint arXiv:1711.05101*, 2017.
- [54] T. Dettmers, M. Lewis, S. Shleifer, and L. Zettlemoyer. 8-bit optimizers via block-wise quantization. *arXiv preprint arXiv:2110.02861*, 2021.
- [55] C. Chen and J. Mo. IQA-PyTorch: Pytorch toolbox for image quality assessment. [Online]. Available: <https://github.com/chaofengc/IQA-PyTorch>, 2022.
- [56] I. Skorokhodov, S. Tulyakov, and M. Elhoseiny. Stylegan-v: A continuous video generator with the price, image quality and perks of stylegan2. In *Proceedings of the IEEE/CVF Conference on Computer Vision and Pattern Recognition*, pages 3626–3636, 2022.
- [57] A. Radford, J. W. Kim, C. Hallacy, A. Ramesh, G. Goh, S. Agarwal, G. Sastry, A. Askell, P. Mishkin, J. Clark, G. Krueger, and I. Sutskever. Learning transferable visual models from natural language supervision. *CoRR*, abs/2103.00020, 2021. URL <https://arxiv.org/abs/2103.00020>.

## A Website and Video

We encourage the readers to open the website <https://cfeng16.github.io/this-and-that/> through their internet browsers. This site hosts our introductory video and various other visual results, allowing a dynamic view of our video-based approach’s versatile and powerful capabilities.

## B Document Overview

In this supplementary document, we provide detailed additional content that complements the main paper. Section C elaborates on details of additional qualitative results and ablation studies for both our proposed Video Diffusion Model (VDM) and Diffusion Video to Action model (DiVA). Section D elaborates on details of our proposed VDM architecture, training details, and automatic gesture labeling methods. Section E elaborates on details of DiVA implementation details. Section F elaborates on details of VDM training, testing, and user study details as well as DiVA training, testing, and simulator environment details. Additionally, we show VDM limitations (Sec. G).

## C Additional Experiments and Ablation Studies

### C.1 Qualitative Comparison with Contemporary Video Generative Models.

In Fig. 8, we present a visual comparison of our method against contemporary video generation models, augmenting the quantitative data presented in Table 1 of the main paper.

AVDC [2] is trained on the entire Bridge dataset, so it produces a semantically correct sequence. However, the visual quality of AVDC’s output is lacking, characterized by low spatial and temporal resolution along with visual artifacts on the microwave door. These deficiencies hinder the accurate interpretation of the end-effector and environmental states, which are critical for translating the videos into robot actions. Other leading video generation models, such as DragAnything [26], StreamingT2V [24], and SVD [1], when used directly without specific fine-tuning, were unable to adhere to the provided text or gesture commands. This underscores the need for a specialized language-gesture VDM, specifically designed for robotic applications.

### C.2 Additional Qualitative Results on Bridge.

In Fig. 7, we present additional qualitative results from our test split of the Bridge dataset. We use the provided initial frame and construct new text and gesture prompts to generate unique videos. It’s important to note that the combinations of prompts and frames in Figure 4 of the main paper and the first example in Fig. 7 do not exist in the original dataset, and there are no corresponding ground truth videos. This approach was chosen because the entire Bridge dataset, including our test split, was used for training the AVDC model, which represents the current state-of-the-art open-source video generator for robotics applications. Our results are compared against both our language-only baseline and the AVDC.

In the first example from Fig. 7, video generators relying solely on language inputs (3rd row) struggle to capture the nuanced geometric relationship implied by the prompts, resulting in implausible video outputs. The second example reveals that both our language-only baseline (6th row) and the AVDC (5th row) were deemed unsuccessful in a user study. Although the AVDC attempted to align with the specified direction on the table, the generation quality was poor, and the blue box became invisible after movement. In the third example, our language-only baselines (9th row) performed well, correctly capturing the straightforward “closing” action. However, the AVDC (8th row) failed to follow the text prompt accurately, likely due to overfitting the training data.

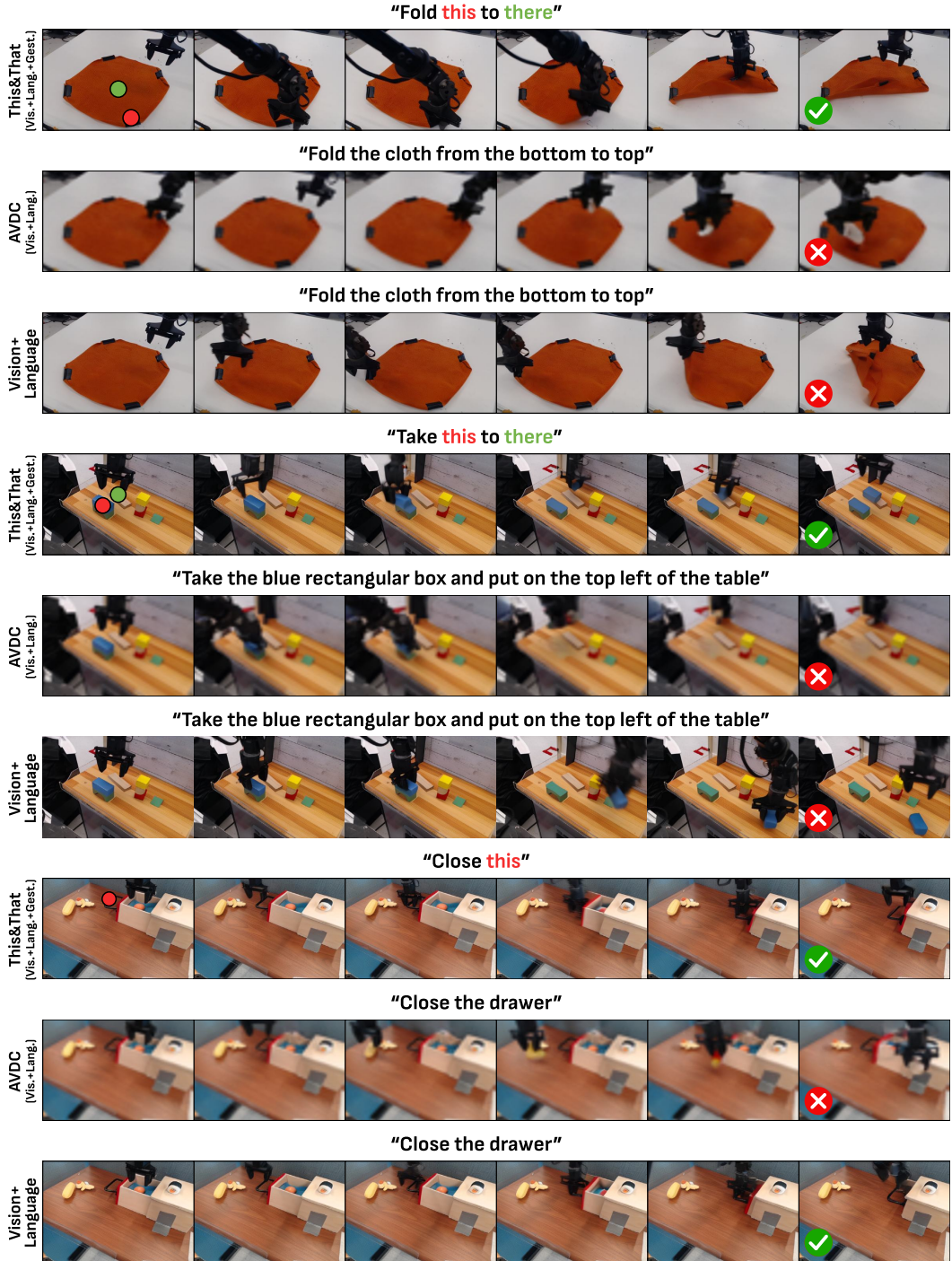


Figure 7: **Video-based Planning Qualitative Results.** We present three examples to compare This&That with AVDC [2] and our VDM baseline conditioned on just the first frame and language. The gesture locations are overlaid in the leftmost frame. Our method can generate action sequences effectively with higher visual quality, even when using deictic words. Note the exceptional quality of our generated videos and the better alignment with the prompts compared to the baselines.

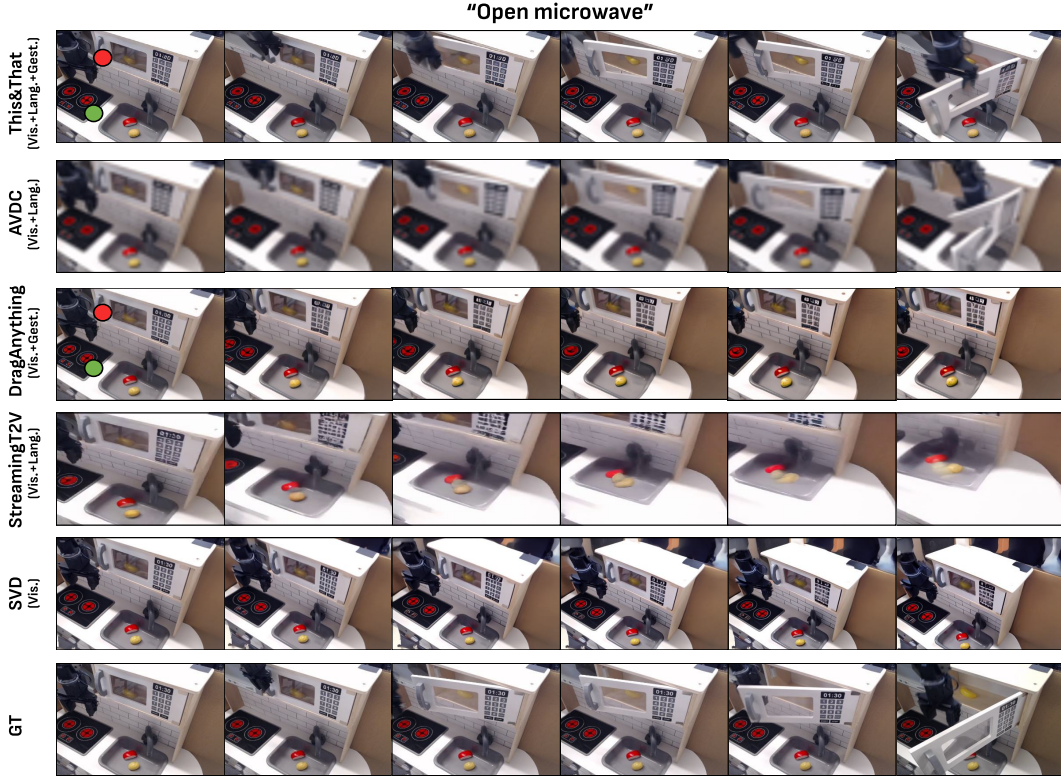


Figure 8: **Qualitative Comparison with State-of-the-art Video Generative Models.** Recent methods such as DragAnything [26], StreamingT2V [24], and SVD [1] fail to generate correct videos following the language or gesture commands. AVDC [2] produces a reasonable result (this scene is part of its training data) but lacks visual quality. *This&That* produces a high-quality video that adheres to the user’s intention.

### C.3 VDM Ablation Study

To validate the design decisions behind our Video Diffusion Model (VDM) architecture, we conducted an ablation study from three distinct perspectives (as illustrated in Tab. 4).

**Assessing Naïve ControlNet Conditioning** Our first ablation revisits the standard ControlNet conditioning architecture. We substituted our proposed approach, which involved pre-trained VAE encoding, with a simple zero convolution, and removed our concatenation method for integrating gesture conditioning and VDM noise inputs. This change significantly reduced performance across all assessed metrics. Visual inspections of the generated videos confirmed that they failed to accurately follow the specified gesture cues, underscoring the superiority of our original concatenation and encoding methods in maintaining adherence to gesture inputs.

**Using Semantic Segmentation Masks in Gesture-Conditioning** The second ablation experiment investigates the usage of segmentation masks during training, which could potentially offer more spatial information during gesture-conditioned training. By querying the SAM [47] with the “pick” gesture location, we can obtain a segmentation mask that provides denser gesture signals. However, this additional spatial information does not translate to improved numerical performance. The segmentation algorithm often misinterprets the intended objects, outputting broader scene segments rather than specific objects, like outputting a desk instead of just the cup on it. This inclusion of extraneous pixel data complicates effective training. Consequently, we found that a simpler approach using 2D dilation from a single point yields better results than employing SAM masks.

| Methods                         | FID↓          | FVD↓          | PSNR↑         | SSIM↑        | LPIPS↓       |
|---------------------------------|---------------|---------------|---------------|--------------|--------------|
| Regular Controlnet              | 22.158        | 124.710       | 18.244        | 0.727        | 0.167        |
| With SAM Segmentation mask      | 17.922        | 88.757        | 19.871        | 0.759        | 0.141        |
| No Layernorm on CLIP Embeddings | 17.566        | 92.527        | 19.758        | 0.759        | 0.142        |
| <b>Ours</b>                     | <b>17.278</b> | <b>84.580</b> | <b>20.029</b> | <b>0.761</b> | <b>0.137</b> |

Table 4: **Ablation study on VDM.** The precision is 3 digits after the decimal point. The best is highlighted.

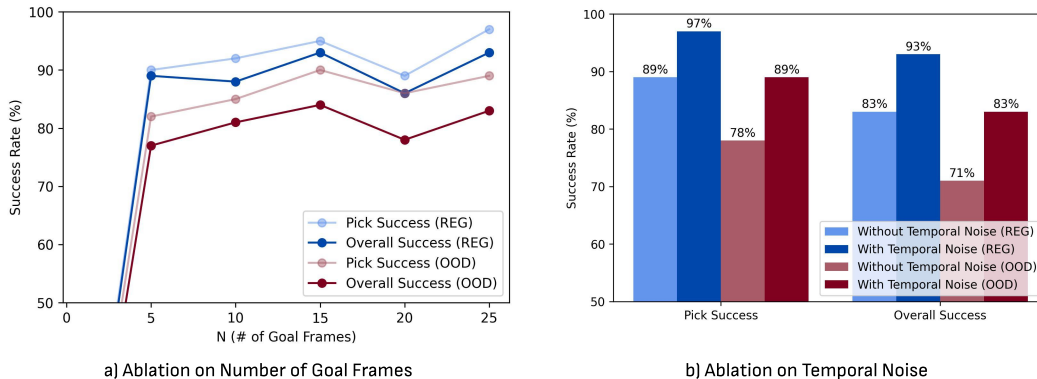


Figure 9: **DiVA Ablation Studies.** We ablate DiVA on a) the number of goal frames (N) and b) the addition of temporal noise during training. DiVA performs best with either 15 or 25 goal frames and with temporal noise.

**Language and First Frame Conditioning** The final ablation focuses on the analysis concerning the cooperation between language and image embeddings using FiLM and cross-attention. Specifically, we empirically find out that the layer normalization layer after concatenating the CLIP embeddings plays an important role in maintaining the video quality: i.e., removing the layer resulted in poorer performance across all numerical metrics.

#### C.4 Additional Qualitative Results from Simulation Rollouts

In Figures 10 and 11, we present further qualitative results from our simulated rollout experiments on Isaac Gym [46]. These results showcase the ability of *This&That* to generate video plans and effectively translate them into robotic actions. While our language-conditioned (without gesture) VDM baseline generally performs well, as evidenced in Table 3 of the main paper, it encounters difficulties with complex sentences involving geometric relations within the context of specific images (see Fig. 10). In particular, when identical objects are presented, the language-only models often fail to generate the correct actions. This issue is notably exacerbated in out-of-distribution tests, such as those depicted in Fig. 11, where all objects involved are identical.

#### C.5 Ablating DiVA: Number of Goal Images and Frame Subsampling Randomization.

We perform two ablation studies for DiVA (Diffusion Video to Action) as shown in Fig. 9. For the first study, we vary N, the number of goal frames we subsample from the generated video frames, from 1 to 25 in increments of 5. We see almost no success for N=1 (conditioning on just the last goal frame), which can be regarded as a baseline for goal-conditioned ACT [4]. The performance increases with the number of conditioning frames, but it plateaus at around N=15 until N=25. We hypothesize that more frames will be beneficial for complex tasks and leave conducting such challenging experiments as future work.

For the second study, we analyze the effects of adding randomness to the subsampling of the goal frames during training. In other words, we split the GT goals into N consecutive groups and randomly



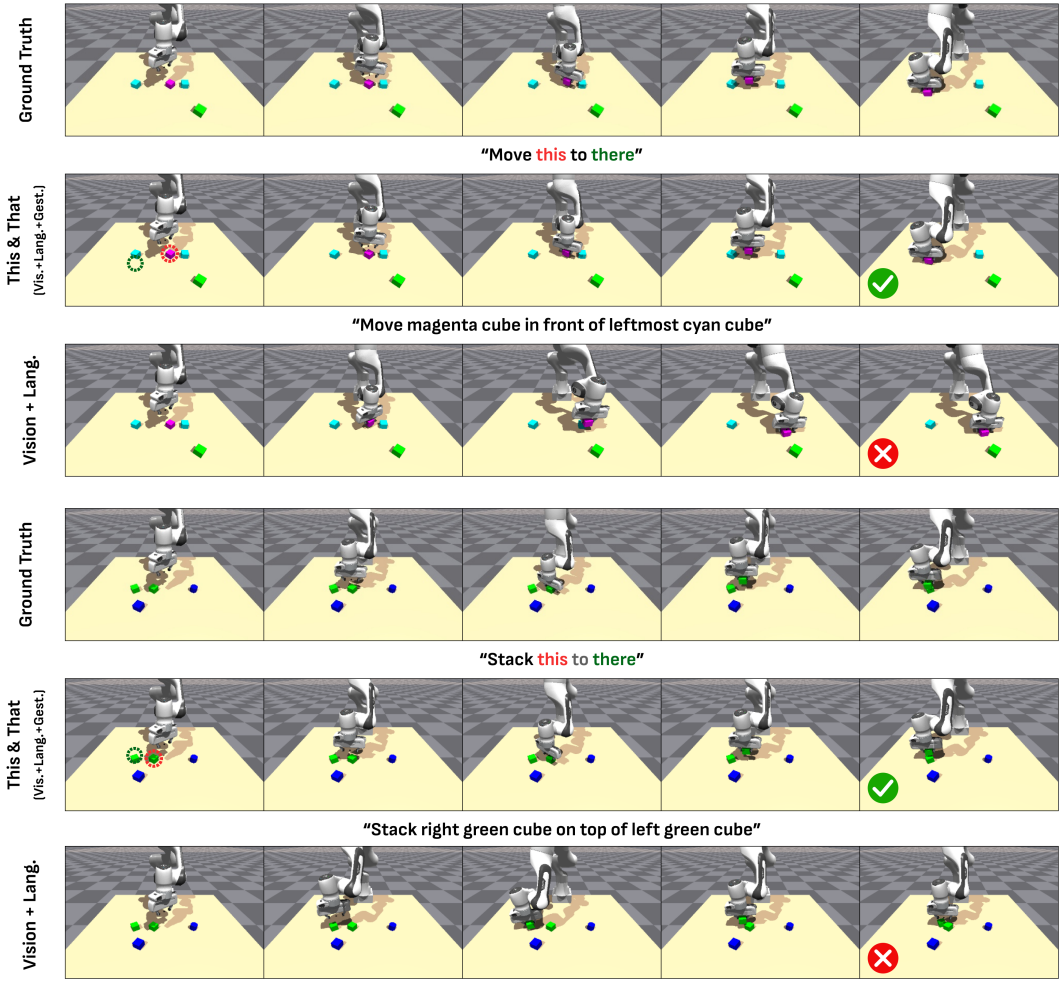


Figure 10: **Simulation Rollout Qualitative Comparison in Regular Scenes.** We compare our language-gesture model against the video-based baseline conditioned solely on language in regular scenes. The language-only VDM struggles to resolve even slight scene ambiguities. In contrast, our model effectively translates user intentions into actions, even with the use of simple deictic words.

sampled one image from each group. We find that implementing this temporal randomness makes DiVA more accurate and robust.

## D Video Diffusion Model Implementation Details

### D.1 Base Architecture

The video diffusion model (VDM) we use is based on the Stable Video Diffusion (SVD) framework [1], which incorporates a modified version of the denoising algorithm from the EDM [48], a continuous-time diffusion model framework. Since the training code of SVD is not publicly available, we first deploy an open-source codebase <sup>1</sup> and make several modifications to the denoise algorithm as described in the following sections.

<sup>1</sup>[https://github.com/pixeli99/SVD\\_Xtend](https://github.com/pixeli99/SVD_Xtend)

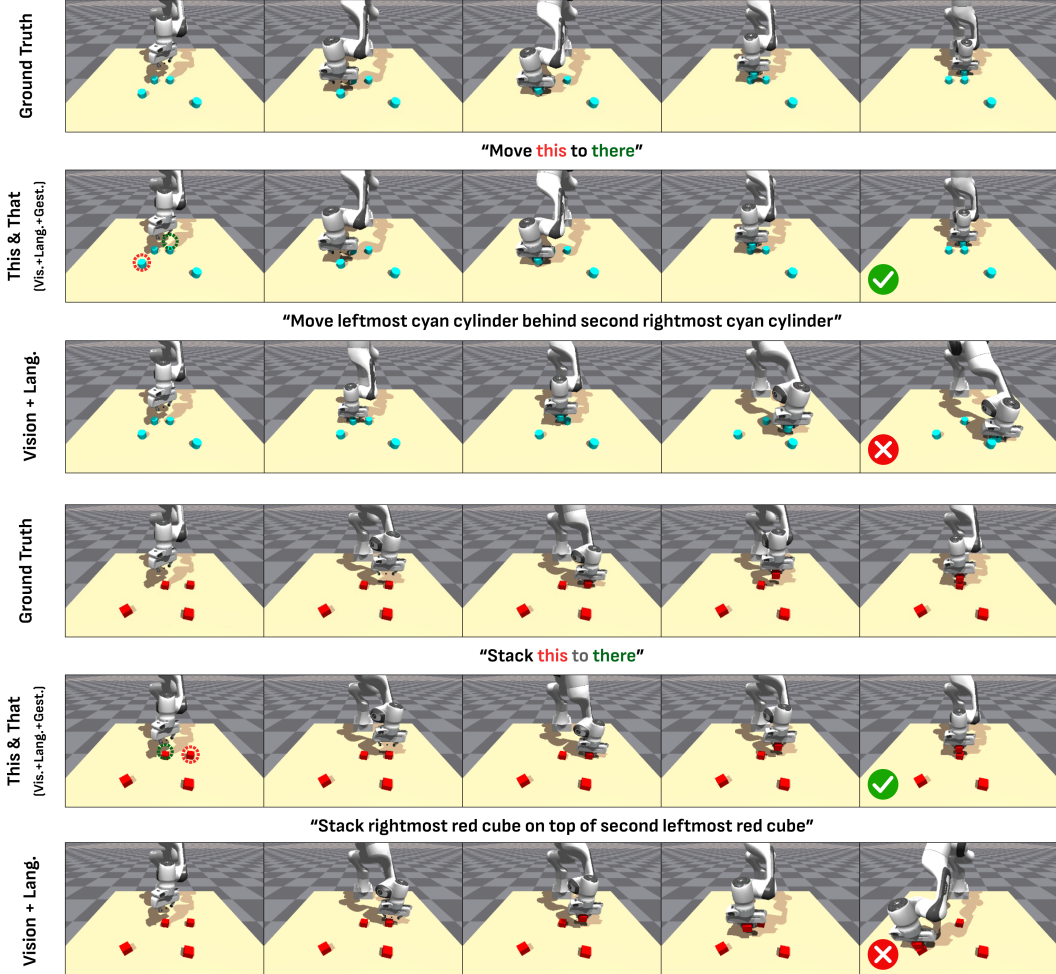


Figure 11: **Simulation Rollout Qualitative Comparison in out-of-distribution (OOD) Scenes.** We compare our language-gesture model against the video-based baseline conditioned solely on language in out-of-distribution scenes with blocks of the same type and color. The language-only VDM struggles to interpret complex text instructions and resolve scene ambiguities. In contrast, our model effectively translates user intentions into actions, even with the use of simple deictic words.

## D.2 UNet Finetuning Details (Stage 1)

The SVD framework governs video motion using two key parameters: the motion bucket ID and noise augmentation. In robotics applications, a complete video sequence is crucial, depicting the robot arm completing its task. Consequently, we set the motion bucket ID to 200 and the noise augmentation to 0.1, both during training and inference, to override motion control from the pretrained model.

Building on the method proposed by [49], we enhance the stability of our VDM by discarding a small amount of noise  $\log \sigma \sim \mathcal{N}(-3.0, 0.5^2)$  traditionally added to the conditioning frame. Instead, we introduce a fixed noise value of 0.1 as an augmentation during training.

For effective text and first frame image conditioning, we concatenate the embeddings prior to their introduction to the encoder hidden states. Given the varying dimensions of text embeddings across different open-source CLIP [39] models, we select a version that matches the feature dimension of our SVD’s CLIP image embeddings, which is 1024. We utilize a CLIP encoder from the StableDiffusion2.1 framework [37] for text embeddings, resulting in dimensions of  $x_{\text{text}} \in \mathbb{R}^{b \times 77 \times 1024}$  and  $x_{I_0} \in \mathbb{R}^{b \times 1 \times 1024}$  for image embeddings, aligning perfectly for concatenation. The final concatenated dimension is  $x_{\text{concat}} \in \mathbb{R}^{b \times 78 \times 1024}$ . We observe that applying Layer Normalization [50] to these

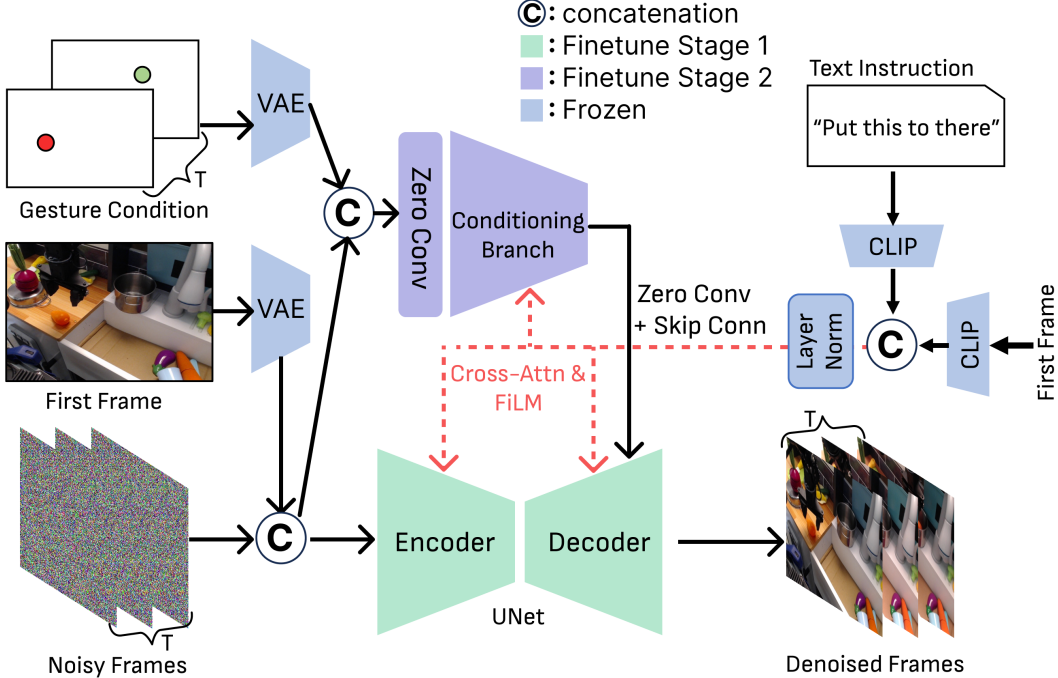


Figure 12: **A detailed visualization of our VDM architecture.** In the first fine-tuning stage, we fine-tune the UNet weights of SVD [1], conditioned on the first frame and the CLIP [39] embedding of the text inputs. In the second stage, we initialize the conditioning branch using the weights from the UNet encoder and attach a zero convolution layer whose weights are initialized to be zero, following ControlNet [40]. Note that the gesture conditioning images are mapped into the latent space and concatenated with the noise and first frame latents. The CLIP embeddings of the first frame and the text prompts are concatenated and processed with layer normalization before being used to modulate the UNet and the conditioning branch with cross-attention and FiLM [38] operation.

concatenated embeddings enhances both the visual and quantitative outcomes of our model as shown in Tab. 4. The processed language and vision encoder hidden states for the diffusion model are then defined as:  $y_{hs} = \text{LayerNorm}([\text{CLIP}(x_{\text{text}}); \text{CLIP}(x_{I_0})])$ .

### D.3 Gesture Conditioning Branch Details (Stage 2)

In the second stage of training for the gesture conditioning branch, we implement temporal conditioning by distributing two gesture points across different frames. For a sequence of  $T$  target frames, only two frames contain gesture point pixel information, while the remaining frames hold zero-value images as placeholders. The frames with gesture points are positioned randomly in the sequence, ensuring that the first (red) point appears temporally before the second (green) point as shown in Fig. 12. Each gesture point is represented as a square box, 10 pixels per side, centered on the specified coordinate. Building on the techniques from MotionCTRL [33], we employ a 2D Gaussian dilation method to enhance the visibility of gesture points.

The inputs for the first convolution layer include noise vector  $\epsilon \in \mathbb{R}^{(B \times T) \times 4 \times H \times W}$ , the encoded initial frame repeated  $T$  times  $\mathcal{E}(C_0) \in \mathbb{R}^{(B \times T) \times 4 \times H \times W}$ , and the gesture condition vector  $\mathcal{E}(C_{\text{gest}}) \in \mathbb{R}^{(B \times T) \times 4 \times H \times W}$ . The dimensions  $(B \times T)$ ,  $H$ , and  $W$  indicate batch size times number of frames, and the height and width of the latent space, respectively. The resulting channel-wise concatenation forms a shape of  $\mathbb{R}^{(B \times T) \times 12 \times H \times W}$ .

Given the discrepancy in input dimensions between the gesture conditioning branch and the UNet’s first convolution layer, we do not reuse the pre-trained convolution layer from the UNet. Instead, we train a new convolution layer from scratch with zero initialization (zero convolution), which helps

mitigate potential issues from random noise gradients during the initial stages of training. Following the concept from Follow Your Clicks [27], we implement latent masking on the gesture conditioning inputs by turning latent features off with some probability  $p$ . This masking technique is applied exclusively on the gesture conditioning side to prevent the performance degradation observed when applied on the UNet side.

The input formulations for the gesture conditioning and UNet in stage two are as follows:

$$y_{\text{Gest}} = \mathcal{Z}([\mathcal{M}_p(\mathcal{E}(I_0)); \epsilon; \mathcal{E}(C_{\text{gest}})]),$$

$$y_{\text{UNet}} = \mathcal{C}([\mathcal{E}(I_0); \epsilon]),$$

where  $\mathcal{Z}(\cdot)$  represents the zero convolution,  $\mathcal{C}(\cdot)$  represents the regular convolution layer, and  $\mathcal{M}_p(\cdot)$  represents the latent mask with probability  $p$ . The  $y_{\text{Gest}}$  vector serves as the input to the conditioning branch encoder, while  $y_{\text{UNet}}$  feeds into the UNet encoder. Note that both the UNet and the gesture conditioning branch intermediate features are modulated using FiLM [38] conditioning, whose parameters are obtained by cross-attending to the CLIP embeddings. We refer readers to the SVD and StableDiffusion implementations for details of this structure. Finally, the conditioning branch is used to provide skip connection values to the UNet decoder following the ControlNet architecture [40].

#### D.4 Automatic Gesture Labeling on Real Data

The Bridge datasets [6, 5] provides metadata of the robot end-effector actions, from which we can recover the key moments when the robot end-effector either closes to grasp or reopens to release objects. Utilizing these temporal markers, our objective is to precisely determine the gripper’s interaction points with objects at these key frames. To facilitate this, we employ a bounding box detector developed through training a YoloV8 [51] model on 450 manually annotated images that mark the gripper’s location. This specialized training enables the model to accurately outline the gripper’s bounding box in subsequent frames, ensuring automatic detection and tracking of its interactions with objects.

With the gripper’s bounding box identified, we extract the 2D coordinates of the objects at the target frame index. We then employ the TrackAnything model [52] to track the objects’ motion over time. This tracking approach is crucial, especially in scenarios where objects are released mid-air by the gripper, necessitating continuous monitoring of their trajectory to determine their landing points. This method reliably provides the two necessary gesture points for our application.

However, this automated annotation method is not infallible. Challenges arise in tracking more complex interactions, and the Yolo model does not achieve perfect detection accuracy. Consequently, we exclude results from cases where tracking accuracy falls below acceptable thresholds. Additionally, we discard videos that exceed five times the length of the target frame count  $T$  or have fewer frames than  $T$ .

To aid the research community in enhancing gripper detection capabilities, we will release both the detection code and the pre-trained weights. For further details and to access these resources, we encourage interested readers to consult our code repository once it is released.

## E DiVA Model Implementation Details

Our Diffusion Video to Action (DiVA) framework is designed to model the distribution  $\pi_{\theta}(a_{t:t+k}|o_t, s_t, \tau)$ , where  $a_{t:t+k}$  represents the action chunk the robot executes from time  $t$  to  $t+k-1$ . Here,  $o_t$  is the image observation of the environment at time  $t$ ,  $s_t$  is the pose of the robot’s end-effector at time  $t$ , and  $\tau$  includes a subset of goal images from the video diffusion model output  $\mathcal{I} := I_{0:T}$ . We denote  $N = |\tau|$  to be the size of the subset. DiVA processes each image of resolution  $\mathbb{R}^{256 \times 384 \times 3}$  through a ResNet-18 architecture, pre-trained on ImageNet and adjusted during training, to produce latent embeddings of shape  $\mathbb{R}^{8 \times 12 \times 512}$ .

The latent embeddings for  $o_t$  and  $\tau$  are then flattened to  $z_{o_t} \in \mathbb{R}^{96 \times 512}$  and  $z_{\tau} \in \mathbb{R}^{N \times 96 \times 512}$ , respectively. To incorporate the temporal dimension of  $\tau$ , fixed 2D sinusoidal positional encodings

of dimension  $\mathbb{R}^{N \times 512}$  (expanded to  $\mathbb{R}^{N \times 96 \times 512}$ ) are added to  $z_\tau$ . The embeddings  $z_{o_t}$  and  $z_\tau$  are subsequently processed by a TokenLearner [41] module, which utilizes spatial attention to select 16 dynamic and significant tokens per feature map, resulting in goal tokens  $G \in \mathbb{R}^{N \times 16 \times 512}$  and 16 tokens of dimension 512 for  $o_t$ . TokenLearner is implemented as a multilayer perceptron (MLP) with LayerNorm and a single hidden layer of 64 units.

Another MLP is used to encode the end-effector pose  $s_t$  into a single token. This token is concatenated with  $o_t$  to form  $O \in \mathbb{R}^{17 \times 512}$ . DiVA then employs a transformer encoder to process  $O$  input with 4 layers of self-attention and cross-attention to the goal tokens  $G$ . This is followed by a transformer decoder applying self-attention to fixed 2D sinusoidal positional embeddings of shape  $\mathbb{R}^{k \times 512}$  across 7 layers of self and cross-attention to the encoder outputs.

The final  $k$  output tokens of the transformer are decoded into the actionable sequence  $a_{t:t+k}$  using a standalone MLP for each token. The full action chunk of size  $k$  is executed before querying the model again. In our experiment, we use  $k = 10$ . We utilize an L1 loss function for training, which ensures greater stability compared to L2 loss. A schematic overview of DiVA’s architecture is detailed in Figure 3 of our main paper.

### E.1 Alternative Method: Inverse Dynamics Model

Initially, we explored training an inverse dynamics model to interpolate actions between frames produced by our video diffusion model, inspired by the methods described in UniPi [34]. However, we observe that such a strategy failed to produce reasonable action outputs, likely because our diffusion model generates a fixed number of frames for each demonstration, whereas the actual demonstrations vary in length. This discrepancy made it impractical to train an inverse dynamics model that could uniformly output a fixed number of actions for each frame sequence without introducing an additional diffusion model dedicated to temporal interpolation as used in UniPi[34]. Our method avoids such additional generative steps and is robust to the number of input images and temporal misalignments as shown in Sec. C.5.

## F Experiment Details

### F.1 VDM Training Details

In the Bridge dataset training, we use 8 Nvidia L40S GPUs with 48 GB memory each to train 99K iterations (the closest checkpoint to 100K iterations) for the UNet and 4 GPUs with 30K iterations to train the gesture conditioning in the second stage. The batch size is 1 for each GPU. The pre-trained weight we start with is the default SVD model for the 14-frame version. For our training on the Isaac Gym dataset, we use 8 GPUs for 30K iterations in the stage 1 and another 4 GPUs for 15K iterations in the stage 2. The pre-trained weight we start with is SVD-XT for the 25-frame version. We apply the AdamW [53] optimizer with a constant learning rate of 1e-5 and 5e-6 respectively for two stages. We apply the 8-bit Adam [54] strategy to decrease GPU memory consumption, and no ema is employed.

To augment the sparsity of the dataset available, we propose a horizontal flip mechanism to augment the dataset. The probability of flipping is 0.45. However, we keep in mind that if the language prompt contains keywords with position meanings, like *left* and *right*, we will not do flipping.

### F.2 VDMs Visual-Quality Experiment Details

The testing dataset is coming from the train-test split on 10% of the data from both V1 [6] and V2 [5] to facilitate subsequent quantitative comparisons. For the VDM table, we apply all 646 videos from Bridge V1 after gesture label filtering.

In the VDM quantitative comparisons, we employ FID [43], FVD [44], PSNR, SSIM, and LPIPS [45] as our numerical metrics. We compute FID by sampling 9,000 images randomly from the generated frames and the ground truth dataset by the codebase of pyiqa [55]. The implementations of FVD,

PSNR, SSIM, and LPIPS are from an open source<sup>2</sup>. FVD uses the inception network provided in StyleGAN-V [56].

All methods first output at the resolution and number of frames available in their codebase and then resize to 256x384 and 14 frames. Specifically, SVD [1] outputs at 256x384 with 14 frames and the motion score is 180 with a noise aug strength of 0.1. StreamingT2V [24] outputs at 1280x720 with 24 frames and the base model we choose is SVD. We only keep the first 14 frames of 24 frames to compare with GT. DragAnything [26] outputs at 576x320 with 14 frames. The two drag points we chose are the same gesture points we applied in our gesture conditioning training. We connect two drag points by a straight line. AVDC [2] outputs at 48x64 with 7 frames and 25 sampling steps in the inference stage and the frames are interpolated to 14 frames by repeat. For our model, we directly output at 256x384 with 14 frames for the Bridge testing.

### F.3 User Alignment Experiment Details

For the human study, we selected three individuals with experience in robotics to evaluate our models. Each participant reviewed independently generated results from *This&That* and other baseline VDMs to minimize the stochasticity of the study stemming from the generative models’ random nature. We selected a total of 24 test cases, divided into specific tasks: 8 cases for pick-and-place, 5 for stacking, 6 for folding, and 5 for opening or closing actions. We prepare video outputs of *first-frame-only*, *first-frame+language*, *first-frame+gesture*, *first-frame+gesture+language* (ours) conditional approaches along with those of AVDC. For methods that use text inputs, we test both deictic and regular versions.

Given that the AVDC model was trained using the entire Bridge v1 and v2 datasets, our traditional train-test split method does not fully assess its capabilities. Instead, we opted to generate entirely new content as conditioning input, which better demonstrates the model’s zero-shot generation abilities. This involved altering the language prompts and gesture points to incorporate different objects to pick up, different placement positions, or both. This approach allows us to more effectively evaluate the model’s adaptability and performance in novel scenarios.

For our human study, participants were presented with an image accompanied by the non-deictic language prompt and gesture points indicating the start and, optionally, the endpoint. We asked evaluators the following question to gauge the alignment of the videos with the ground truth intentions:

*”Given one image with the stated intention through a language prompt and gesture points, do you think the generated videos correctly complete the task and align with our intentions?”*

#### F.3.1 Preparing Deictic Language Prompts

The deictic language prompts are generated by automatic scripts that prepend the first action verb to the phrase “*this to there*”, resulting in prompts like “*put this to there*”, “*fold this to there*”, and “*stack this to there*”. These deictic text prompts, despite their ambiguity, are tested for zero-shot capability using the same model weights trained on regular text conditions. Through our experiment, we explore whether simplistic deictic language, such as “*this*” and “*there,*” affects the clarity and alignment of the video generation.

#### F.3.2 Training Details of the VDM Baselines

- Vision Model: Utilizes the UNet from Stage 1 designed for the image-to-video task, operating independently of any text prompt.
- Vision+Language Model: This version of the UNet, also from Stage 1, incorporates both image and text prompts to generate videos.
- Vision+Gesture Model: Employs the temporal ControlNet from Stage 2, using the vision model’s pre-trained weights as its backbone.

---

<sup>2</sup>[https://github.com/JunyaoHu/common\\_metrics\\_on\\_video\\_quality](https://github.com/JunyaoHu/common_metrics_on_video_quality)

- Vision+Language+Gesture Model: Integrates gesture conditioning training from Stage 2, leveraging the pre-trained UNet weights from the Vision+Language model.
- The AVDC model, which inherently accepts image and text prompts as input, was utilized directly with its pre-trained weights for inference to evaluate its effectiveness under the above configurations.

#### F.4 DiVA Training Details

We train DiVA using 900 instances for training and 100 instances holdout for testing. Each demonstration consists of approximately 75-100 observation, action pairs. We use a single Nvidia RTX 6000 Ada GPU for 2,000 epochs, which is the same quantity as ACT [4]. We save checkpoints every 500 epochs and use the checkpoint with the lowest validation error during evaluation. During training, we only use goals sampled from the ground-truth (GT) data. In other words, we subsample the GT visual observations to obtain goals instead of training directly on the generated videos. This is because we retain high performance with such methods. Thus, we can conclude that there is very little domain gap between GT goals and the videos we generate. For our hyperparameters, we use a batch size of 8, a learning rate of  $1e^{-5}$ , a weight decay of  $1e^{-4}$ , and an action chunk size of 10.

#### F.5 Simulation Experiment Details

Our dataset consists of pick-and-place demonstrations with four blocks on a tabletop environment. Our blocks are composed of two shapes (cube and cylinder) and eight colors (red, blue, green yellow, magenta, cyan, grey, and black). Demos are generated by relating two randomly selected blocks using five variations: *in front of*, *behind*, *to the right of*, *to the left of*, and *on top of*. We classify the first four relations as *near* tasks and the last as a *stack* task. An example of a language instruction would be *stack the magenta cylinder on top of the black cube*. To show where our method shines, we also create a custom test set with out-of-distribution scenes that contain identical objects in identical colors. In these scenes, we show it is difficult to use language to precisely define the task and is easier to use gesture instead.

All demos are collected using a scripted policy. Actions are 6D delta end-effector pose commands represented in the end-effector frame. An additional continuous scalar between -1 and 1 is appended to the action to indicate whether to open or close the gripper. During inference (rollout), we execute the full action chunk before querying the model again. Our success metrics are also scripted using a set of basic rules. For pick success, we record the maximum vertical displacement that the object to be picked achieves during rollout. If this value exceeds a block diameter for more than 5 timesteps, we consider the pick to be successful. We divide place success into two separate criteria for near and stack tasks. At each timestep, we calculate the planar and vertical distance from the picked object to its goal location. For near tasks, we count place success if the planar distance to goal is within 3 block diameters and the vertical distance to goal is within a block radius. For stack tasks, we count place success if the planar distance to goal is within a block diameter and the vertical distance to goal is within a block radius. The robot achieves overall success if it has achieved both pick and place success. We rollout actions for 250 timesteps, terminating 5 timesteps after the first instance of overall success. For near tasks, we use more lenient metrics since 2D gestures has some 3D ambiguity. In our experiments, a block diameter of 5cm is used.

##### F.5.1 Baseline Details of the Rollout Experiment

In Table 3 of our main paper, we provide simulation results for five models. In the first row, we train vanilla ACT [4] without any goal-conditioning. For the second row, we condition ACT on language by concatenating the CLIP [57] embedding of our language with the image tokens of the current image observation, where the position embeddings for the CLIP is zero-value as a placeholder. For the third row, we condition ACT on both language and gesture. The gesture condition is encoded and position encoded with ResNet in the same way as the current image observation and all the tokens are concatenated together. For the fourth row, we train a VDM with only the first frame



Figure 13: **Object Appearance Artifact.** Occasionally, our method generates a video where the object being moved changes its appearance over time, even though the video closely adheres to the user’s intention. We believe this issue comes from the inherent limitations of representing 3D geometric relationships within 2D video media.

(vision) and language conditioned to mimic prior works [3, 36, 35, 34]. We feed these generated videos to DiVA to generate robot actions. For the fifth row (our contribution), we train a video diffusion model that is conditioned on the first frame (vision), language, and gesture. We feed these generated videos to DiVA again to generate robot actions. Results on both the regular test set and the out-of-distribution (OOD) test set are provided for all models. As shown in Fig. 10 and Fig. 11, the model with Vision+Language+Gesture outperforms all other models, especially when the scenes are ambiguous and OOD.

### **G Limitation: Changes in Object Appearance Over Time**

While our Video Diffusion Model (VDM) framework typically generates high-quality videos, it occasionally alters the shape of objects being moved over time, as shown in Fig. 13. We suspect that this issue stems from the inherent limitations of representing 3D geometric relationships within 2D video media. Nevertheless, we believe that these artifacts might not hinder the translation to robotic actions, as long as the visuals of the end-effector remain clear and discernible.